Journal of Theoretical Biology 414 (2017) 120–127

Contents lists available at ScienceDirect

Journal of Theoretical Biology

journal homepage: www.elsevier.com/locate/yjtbi

An updated kernel-based Turing model for studying the mechanisms of biological pattern formation

Shigeru Kondo

Graduate School of Frontier Biosciences, Osaka University, 1-3 Yamadaoka, Suita, Osaka 565-0871, Japan

ARTICLE INFO

Keywords:
Turing pattern
Reaction-diffusion model
Pattern formation
Kernel
Pigmentation pattern
Zebrafish
LALI model

ABSTRACT

The reaction-diffusion model presented by Alan Turing has recently been supported by experimental data and accepted by most biologists. However, scientists have recognized shortcomings when the model is used as the working hypothesis in biological experiments, particularly in studies in which the underlying molecular network is not fully understood. To address some such problems, this report proposes a new version of the Turing model.

This alternative model is not represented by partial differential equations, but rather by the shape of an activation-inhibition kernel. Therefore, it is named the kernel-based Turing model (KT model). Simulation of the KT model with kernels of various shapes showed that it can generate all standard variations of the stable 2D patterns (spot, stripes and network), as well as some complex patterns that are difficult to generate with conventional mathematical models. The KT model can be used even when the detailed mechanism is poorly known, as the interaction kernel can often be detected by a simple experiment and the KT model simulation can be performed based on that experimental data. These properties of the KT model complement the shortcomings of conventional models and will contribute to the understanding of biological pattern formation.

1. Introduction

The reaction-diffusion (RD) model presented by Alan Turing in 1952 (Turing, 1952) is a theoretical mechanism to explain how spatial patterns form autonomously in an organism. In his classic paper, Turing examined the behaviour of a system in which two diffusible substances interact with each other, and found that such a system is able to generate a spatially periodic pattern even from a random or almost uniform initial condition. Turing hypothesized that the resulting wavelike patterns are the chemical basis of morphogenesis.

Although Turing's theory was not sufficiently supported by experimental evidence for many years (Meinhardt, 1995), it has since been adapted by many mathematical researchers who showed that a wide variety of patterns seen in organisms can be reproduced by the RD model (Meinhardt, 1982; Murray, 2001). Meinhardt and Gierer stated that the condition of "local activation with long-range inhibition (LALI)" is sufficient for stable pattern formation (Gierer and Meinhardt, 1972). This indication was quite important because it suggested that other effects on cells (for example, cell migration, physical stress, and neural signals) could replace the effect of diffusion in the original Turing model. Many different models have been presented to account for situations in which diffusion might not occur (Belintsev et al., 1987; Budrene and Berg, 1995; Swindale, 1980; Wearing et al., 2000). However, in all cases, LALI is the anticipated set of conditions sufficient to form the periodic pattern, and the pattern-formation ability is similar. Therefore, these models are also called LALI models (Oster, 1988).

The importance of the Turing model is obvious (Maini, 2004), in that it provided an answer to the fundamental question of morphogenesis: "how is spatial information generated in organisms?". However, most experimental researchers were sceptical until the mid-90s because little convincing evidence had been presented (Meinhardt, 1995). In 1991, two groups of physicists succeeded in generating the Turing patterns in their artificial systems, which showed for the first time that the Turing wave is not a fantasy but a reality in science (Blanchedeau et al., 2000; Ouyang and Swinney, 1991). Four years later, it was reported that the stripes of colour on the skin of some tropical fishes are dynamically rearranged during their growth in accordance with Turing model predictions (Kondo and Asa, 1995; Yamaguchi et al., 2007). Soon after, convincing experimental evidence claiming the involvement of a Turing mechanism in development has been reported (Hamada, 2012; Maini et al., 2006; Muller et al., 2012; Sheth et al., 2012), and in some cases, the candidate diffusible molecules were suggested. Currently, the Turing model has been accepted as one of the fundamental mechanisms that govern morphogenesis (Green and Sharpe, 2015; Kondo and Miura, 2010).

On the other hand, experimental researchers have pointed out problem that occur when the LALI models are used as the working hypothesis. For instance, LALI models can exhibit similar properties of pattern formation despite being based on different cellular and molecular functions (Oster, 1988). Therefore, the simulation of a model rarely helps to identify the detailed molecular mechanism

http://dx.doi.org/10.1016/j.jtbi.2016.11.003
Received 15 July 2016; Received in revised form 1 November 2016; Accepted 5 November 2016
Available online 10 November 2016

(Economou and Green, 2014). Even when a pattern-forming phenomenon is successfully reproduced by the simulation of an RD system, it does not guarantee the involvement of diffusion. This problem is quite serious because, in most experimental uses, the key molecular event that governs the phenomenon is unknown when the experimental project begins.

It has also become clear that the pre-existing LALI models cannot represent some real biological phenomena. In the formation of skin pigmentation patterns in zebrafish, the key factors are cell migration and apoptosis induced by direct physical interaction of cell projections (Hamada et al., 2014; Inaba et al., 2012; Yamanaka and Kondo, 2014). This is not the only case in which the key signals for pattern formation are transferred not by diffusion but by fine cell projections such as filopodia (De Joussineau et al., 2003; Sagar and Wiegreffe, 2015; Vasilopoulos and Painter, 2016), which may be essentially different than signalling by diffusion. In diffusion, the concentration of the substance is highest at the position of the source cell and rapidly decreases depending on the distance from the source. Therefore, it is difficult to use diffusion to model the condition in which the functional level of the signal has a sharp peak at a location distant from the source (Fig. 1). As each LALI model is restricted by its assumed signalling mechanism, it is difficult to adapt a model to an arbitrary stimulation-distance profile of a real system. In this report, I present a new version of the Turing model that complements the shortcomings of conventional models.

2. Model concept and description

In the modelling of systems that include non-local interactions, the integral function is useful. For example, in the case of a neuronal system, the change of firing rate n at position x is represented by

$$\frac{\partial n}{\partial t}=f(n)+\int w(x-x')n(x',t)dx' \quad (1)$$

(Murray, 2001)(2nd ed. Section 11).

Here, $w(x\text{-}x')$ is the kernel function, which quantifies the effect of the neighbouring $n(x',t)$ on $n(x,t)$ depending on the spatial distance. In this model system, the shape of the kernel determines how the system behaves. The Fourier transform (FT) of the kernel produces the dispersion relation, which shows the unstable (amplifying) wavelength. Importantly, this kernel method can be used to model the effect of long-range diffusion that results from a local interaction. Murray proposed that "this approach provides a useful unifying concept" (Murray, 2001). The LALI condition can be considered the kernel shape that makes stable waves. Thus, one simple method to generalize the conventional Turing or LALI models would be to directly input an arbitrary kernel shape not based on the assumption of any concrete molecular or cellular events. Such a model can be called a kernel-based Turing model (KT model).

As the KT model is not based on any specific behaviour of the molecules or cells, it is more abstract than the pre-existing mathematical models. However, it is practically useful because the shape of the interaction kernel can be easily measured by some simple experiment in some cases. For example, in the case of the pigmentation pattern in zebrafish, in which the mutual interactions between melanophores and xanthophores form the pattern (Nakamasu et al., 2009), we ablated a group of xanthophores with a laser and observed the increase or decrease in melanophores in the neighbouring and distant regions. The data that can be obtained by this simple experiment is a activation-inhibition kernel in itself, and is sufficient to explain how the pattern is made (Nakamasu et al., 2009). Similar experiments could be performed in many different systems to obtain a kernel shape without any information about the signalling molecules.

Consistent with the original Turing model and the models of Gierer and Meinhardt, KT model incorporates the concentration of substance u. u is synthesized depending on the function of cell-cell interaction S, and is destroyed at the constant rate deg, as follows.

$$\frac{\partial u}{\partial t}=S-deg*u \quad (2)$$

The concentration u can be replaced by some activity of the cell. In such cases, deg represents the decay rate of the substances.

The function $Kernel$ is represented by the addition of two Gaussian functions, $A(x)$ and $I(x)$. $A(x)$ and $I(x)$ correspond to the activator and inhibitor in the Gierer-Meinhardt model, respectively (Fig. 2).

$$Kernel(x)=A(x)+I(x) \quad (3)$$

If each cell sends the signal that stimulates or inhibits the synthesis

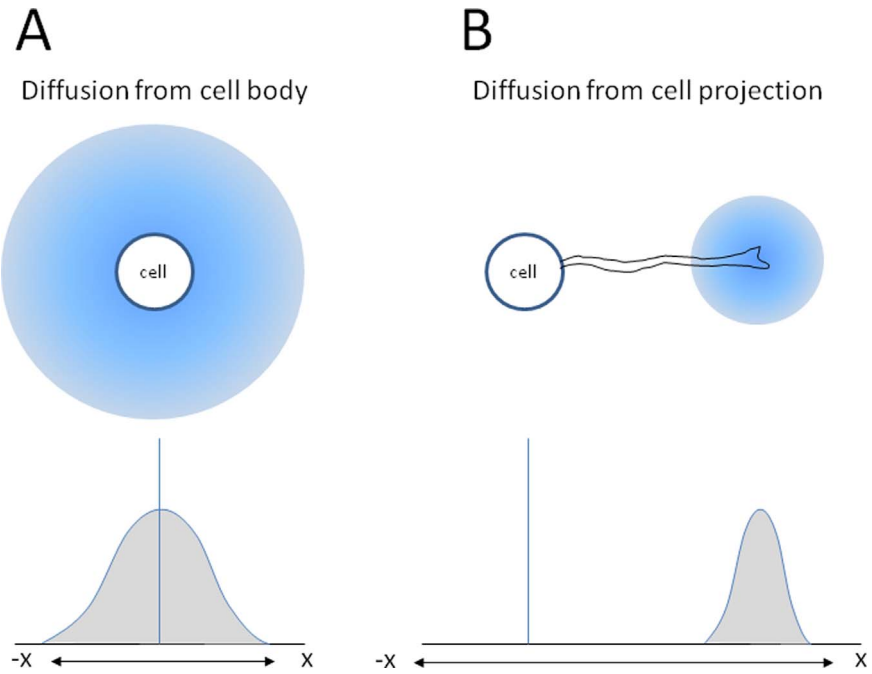

Fig. 1. Interaction strength profiles depend on the method of signal transfer. A: In case of the signal by diffusion, the interaction strength is highest at the source(cell) position. B: If the signal molecule is released at the specific position of a cell projection, the peak of the interaction strength is distant from the source(cell) position.

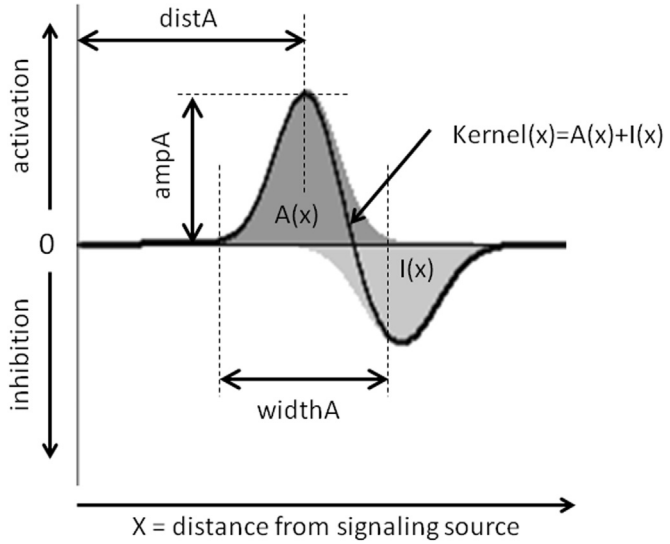

Fig. 2. Definition of the Kernel shape. Kernel function is determined by the addition of two Gaussian functions that can be modified by three parameters: amplitude (ampA and ampB), width (widthA and widthB) and distribution (distA and distB).

of u, the sum of the stimulation received by a cell at position (p,q) is determined by:

$$Stim(p, q) = \iint u(p-\xi, q-\eta) * Kernel(\sqrt{\xi^2 + \eta^2})\, d\xi d\eta \quad (4)$$

In each cell, u is synthesized at a rate of $Stim$. To avoid the synthesis of negative or unusually high levels of u, the lower and upper limits were set as:

$$S(p, q) = \begin{cases} 0, & Stim(p, q) < 0 \\ Stim(p, q), & 0 \le Stim(p, q) < MaxS \\ MaxS, & MaxS < Stim(p, q) \end{cases} \quad (5)$$

The display of the simulation program that calculates the system described above is shown in Fig. 3. The field for pattern formation is a 200×200 array of cells. The maximum interaction distance is 20 cells. The user can alter the parameters of the Gaussian functions using the user-friendly graphical user interface. The FT of the "1D" kernel is also indicated, which helps to deduce the resulting pattern. The software can be downloaded from the journal HP and Kondo's HP. (http://www.fbs.osaka-u.ac.jp/labs/skondo/simulators/KernelPatternGeneraterGauss_Web/KernelPatternGeneraterGauss.html).

3. Results

3.1. Pattern formation by classical LALI conditions

To begin examining the properties that drive pattern formation in the KT model, the LALI condition was modelled. Specifically, the position of interaction peaks (*distA* and *distI*) were set at 0; the dispersion of A (*widthA*) was adjusted to be narrower, and that of I (*widthI*) wider; and the amplifications *ampA* and *ampI* were set to adjust the 2D integrated value of the kernel to approximately 0 (Fig. 4A). I then examined whether the KT model could generate the same pattern as that generated by LALI models.

Using these conditions, periodic patterns form autonomously and are similar to those seen in the simulation of RD and LALI models. The wavelength of the generated pattern corresponds to the peak positions in the FT of the 1D kernel (Fig. 4B, arrow). By slightly changing the values of *ampA* and *ampI*, three basic versions of the pattern (spots, stripes, and networks) emerge (Fig. 4C). All of these properties showed that the pattern-forming properties of the KT model are compatible with that of LALI models.

3.2. Pattern formation by variations on LALI conditions

I next examined pattern formation when the peak position of $I(x)$ was offset from 0 (Fig. 5A). This condition also satisfies LALI, and a periodic pattern emerged as in the classical LALI model (Fig. 5B and C).

Next, by exchanging the $A(x)$ and $I(x)$ functions, I established an inverted LALI condition that has not been tested in the previous study of LALI models (Fig. 5D). This inverted LALI condition gave rise to a periodic pattern with a smaller wavelength (Fig. 5F). The reason is clear from the FT graph; by setting the peak position larger than zero, the FT graph shows a wave pattern. Inversion of the kernel causes the emergence of a new peak at a different position (Fig. 5B and E, arrows). We can conclude from this result that LALI is not a necessary condition for the formation of periodic patterns.

Some biological examples seem to correspond to this case. In some aquarium fish subjected to selective breeding, the wavelength of the pigmentation pattern varies extensively among the breed (Fig. 6A, B). To account for this phenomenon with the conventional RD model requires setting extremely different diffusion rates for each breed. However, because these fish belong to the same species, the mechanism that forms the pattern should be almost the same, and therefore this assumption is biologically quite unlikely. By assuming that the signal transduction has an effective peak at a distant region from the source cell, it is possible to generate patterns of extensively different wavelengths by making only slight changes to the parameter values.

3.3. Nested pattern formation

By setting the peak positions of both $A(x)$ and $I(x)$ distant from zero, the FT of the kernel shows a wave pattern and multiple peaks emerge. When a 2D pattern is calculated with these conditions, in most cases, the dominant wavelength dictates the pattern and thus a periodic pattern resembling that with a single wavelength emerges (data not shown). However, by tuning the parameters, it is possible to generate a nested pattern with two or more wavelengths (Fig. 7A–C). Interestingly, very similar nested patterns are found in some fish species (Fig. 7D, E).

3.4. Identification of the primary factor that determines the variety of 2D patterns

The RD and other LALI models are able to generate a variety of 2D patterns, namely spots, stripes, and networks, and previous studies have examined the parameter sets that give rise to these patterns for each specific model. However, because each model is built on different assumptions of the behaviours of molecules and cells, little is known about the primal factor that controls the 2D pattern. I tested a number of different kernel shapes with the KT model, and in all cases, the determinant of the 2D shape of the waves was the integrated value of the 2D kernel. By setting the integrated value close to zero, stripe patterns emerge irrespective of the kernel shape, while spots always emerge at smaller integrated values and inverted spots (networks) emerge with larger integrated values (Fig. 8A–C). This result persisted when rectangular waves, trigonometric functions, or polygonal lines were used as the kernel shape. This strongly suggests that the primal factor that determines the shape of the 2D wave pattern is the integrated value of the kernel function.

4. Discussion

4.1. Characteristics of the KT model

Unlike the RD and other LALI models, the KT model does not

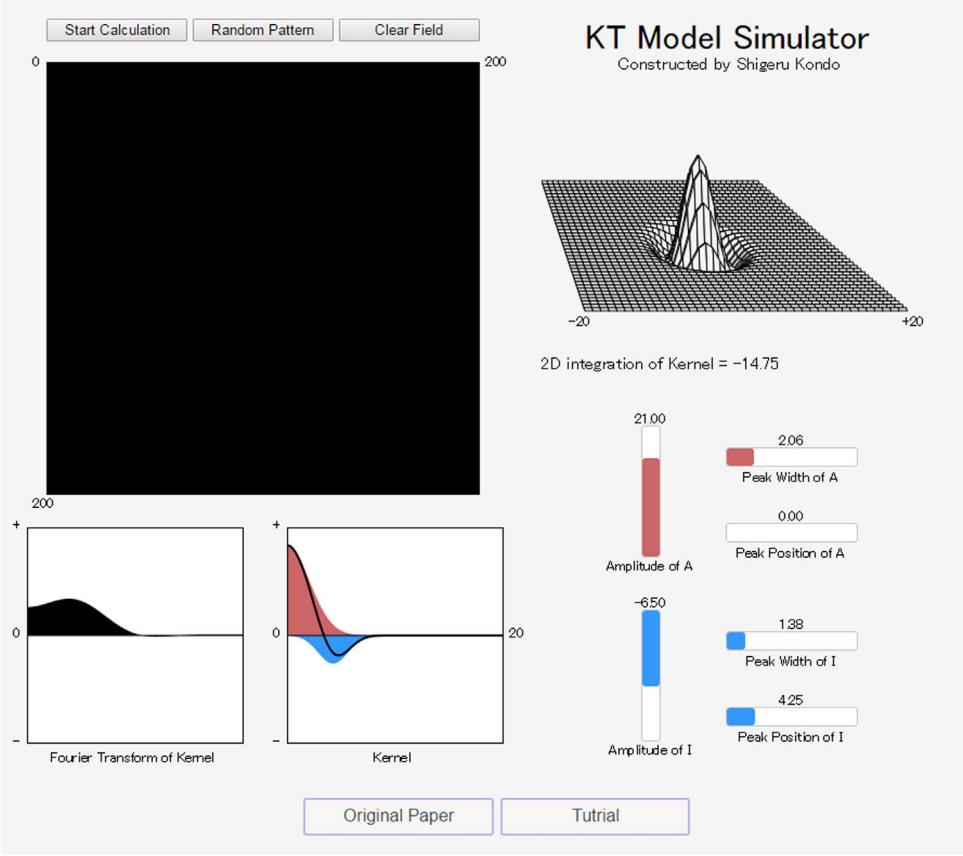

Fig. 3. Display of the KT model simulator. User can change the parameters of two Gaussians with slider controller. The program automatically calculates and shows the 1D and 2D kernel, and the FT of the kernel. Resulting 2D pattern is shown in the big 2D window. As KT model simulator is coded with Java Script, users can run it in the web browsers (Internet explorer, Google Chorme, Safari, etc) visit to following HP. (http://www.fbs.osaka-u.ac.jp/labs/skondo/simulators/KernelPatternGeneraterGauss_Web/KernelPatternGeneraterGauss.html).

assume any mechanisms of molecules or cells, but directly uses an input activation-inhibition kernel. Because of its abstract nature, the KT model cannot predict the detailed molecular or cellular processes involved in the pattern formation. However, as shown in this report, the kernel shape itself provides enough information to explain the formation of various stable patterns. Moreover, the simplicity of the KT model confers some significant advantages that complement the shortcomings of conventional mathematical models.

4.2. Usage of the KT model in experimental studies

Different LALI models that postulate different molecular or cellular mechanisms can sometimes form very similar patterns. Therefore, even if a biological pattern is reproduced by the simulation of a specific LALI model, it does not guarantee that the molecular mechanism anticipated in the model underlies the biological system. Even with recent advances in technology and experimental methods, it is still difficult to identify every part of a molecular network that is involved in formation of a biological pattern. Especially at the beginning of an experimental project, little molecular information is usually available. In most cases, therefore, it is quite difficult to construct a pattern-formation simulation on the basis of reasonable experimental data. These problems led Greene and Economou to question the efficacy of RD and LALI models in the experimental research of morphogenesis (Economou and Green, 2014).

As the KT model is not based on any specific molecular mechanism, it likewise cannot be used to make molecular-level predictions. However, KT model simulations can be performed with a sufficient experimental basis because it is easier to detect the kernel shape. For example, the pigmentation pattern of zebrafish skin is generated by an array of black melanophores and xanthophores that mutually interact. Using laser ablation to kill the cells in a particular region, we measured the increase and decrease of cell density at nearby and distant regions (Nakamasu et al., 2009). The data obtained from this simple experiment is the kernel itself, which is sufficient to predict the development of 2D patterns. In that previous paper (Nakamasu et al., 2009), we used the conventional RD model. However, it was later discovered that the signals are not transferred by diffusion but by the direct contact of cell projections. Because the condition of LALI is retained by both types of projections (long and short), the predictions made by the simulation were correct. However, using an RD model for a system that does not involve diffusion is theoretically contradictory. Using kernel-based simulation can avoid this problem. Kernel detection is also feasible in many other systems. Using light-gated channels or infrared light, for example, one can stimulate, inhibit, or kill cells located at an arbitrary region, and observe the subsequent changes in surrounding cells by live-cell imaging. Therefore, in many cases where the detailed molecular mechanism is unknown, using the KT model should still be safe and practical.

4.3. Usage of the KT model in theoretical analysis

In a simple RD model with two substances, the necessary conditions for stable pattern formation are analytically induced. However, the number of elements (molecules and cells) involved in real pattern-formation events usually far exceeds two. In such cases, the applicability of the LALI concept is uncertain. In fact, some recent computational studies reported that mathematical models of three substances were able to form stable periodic patterns using the reversed LALI condition (Marcon et al., 2016; Miura, 2007). Therefore, the concept of

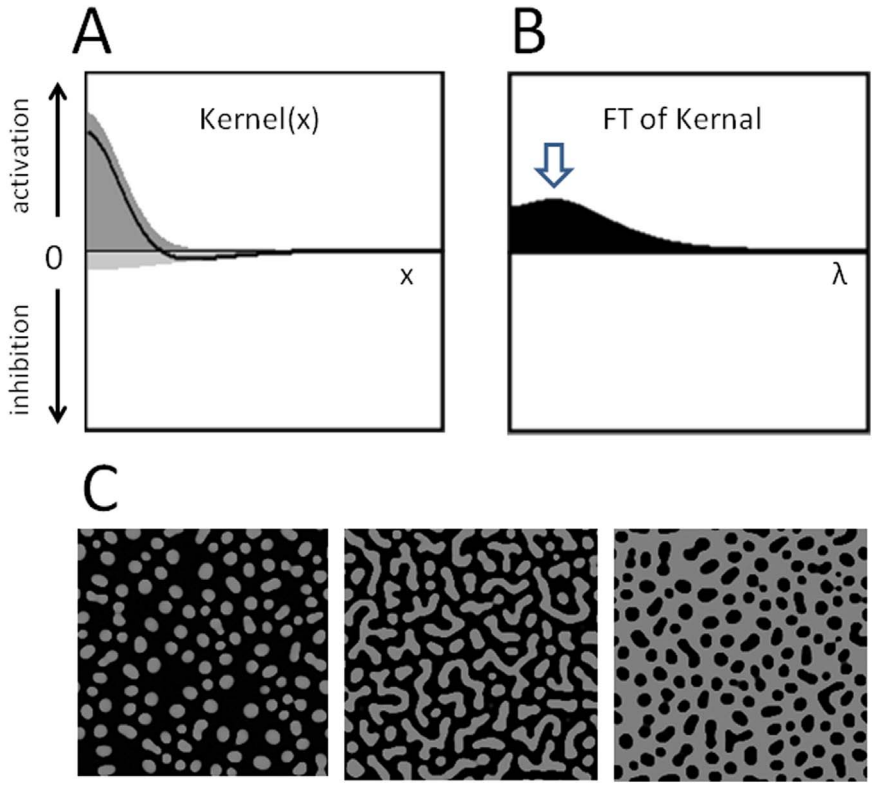

Fig. 4. Pattern formation by LALI conditions. A: The graph of the kernel that s equivalent to the condition of LALI. Gaussian distribution for activator and inhibitor are represented by dark gray and light gray pattern. The kernel (addition of two Gaussians) is represented by the black line. B: Fourier transform of the kernel. Arrow indicates the peak position that represents the spatial frequency of emerging pattern. C: Generated patterns with slightly different parameter sets. (see Parameter Settings for details). Random pattern is used as the initial condition.

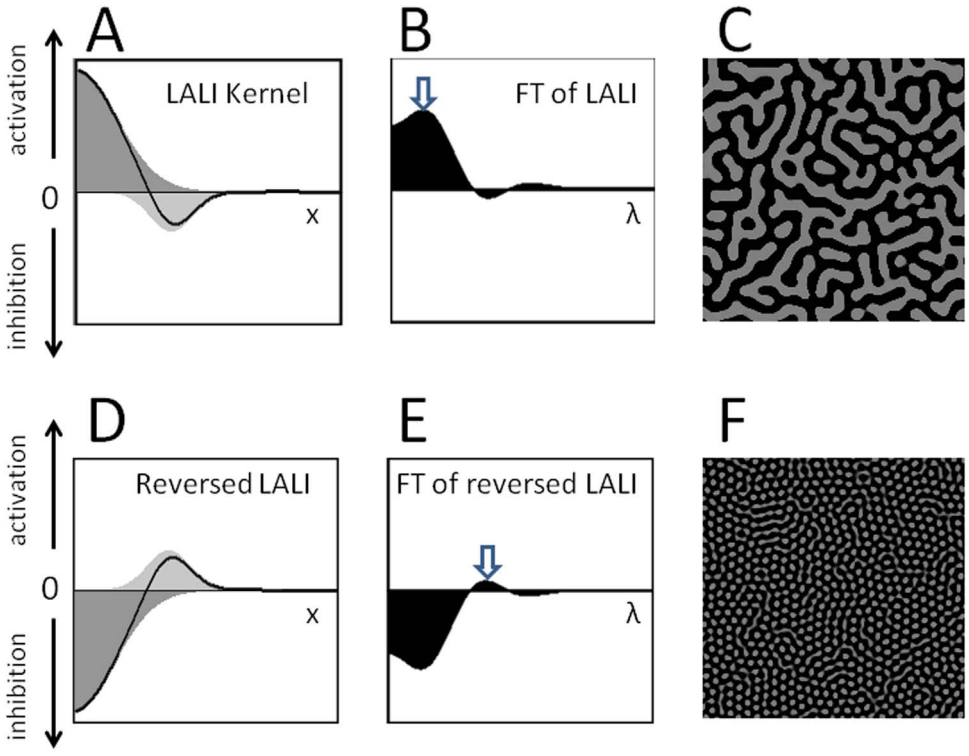

Fig. 5. Pattern formation by non-LALI conditions. A, B and C: Stable pattern formation with LALI condition. D, E and F: Stable pattern formation with inverted LALI condition. See Parameter Settings for details. Random pattern is used as the initial condition.

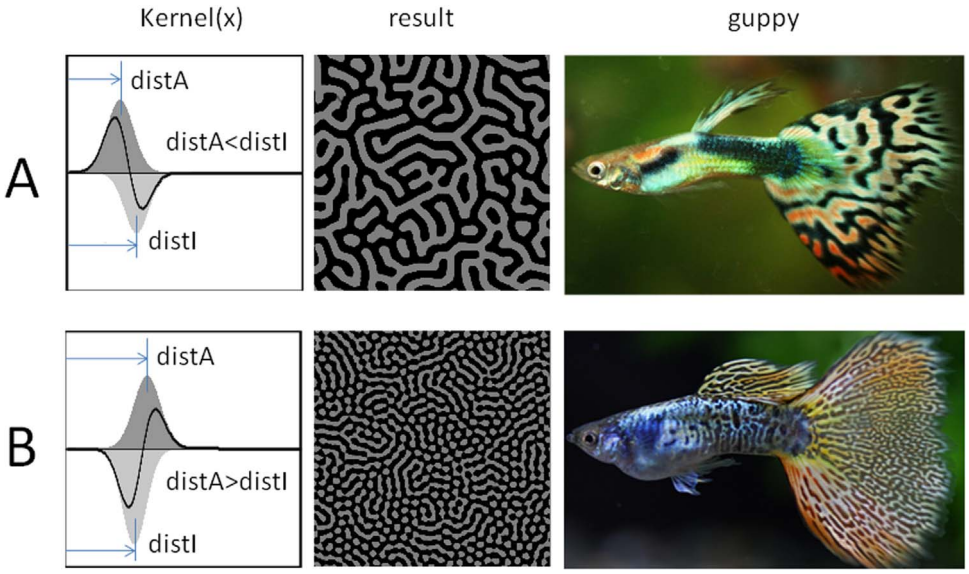

Fig. 6. Simulation of guppy pattern formation. A: When functional distance of the inhibitor is larger than that of the activator ($p < q$), the system generates a wide stripes. B: When functional distance of inhibitor is larger than that of activator ($p > q$), the system generates a drastically finer pattern. Artificial lines of guppy often show such difference in the wave length although they belong to a same species. See Parameter Settings for details. Random pattern is used as the initial condition.

LALI is likely not sufficient to analyse a realistic system with more than three factors. To identify more generalized conditions for the pattern formation, mathematical unification of the various patterning mechanisms may be required. As Murray suggested (Murray, 2001), the kernel concept may be useful for this unification. As shown in this report, the variety of 2D patterns generated by the KT model is wide enough to cover most known biological patterns. Patterns formed by the reversed LALI condition (Marcon et al., 2016; Miura, 2007) can also be reproduced by the KT model. Moreover, the simulation result of KT model (Fig. 7) shows that it can generate some complex spatial patterns that is difficult to be made by conventional models. Nested patterns appear often on the animal skin and sea shells. To reproduce such patterns, conventional models needed to combine two sets of Turing systems (Meinhardt, 2009) or to function a RD system twice at the different time point of its growth (Liu et al., 2006). With the KT model, adjusting the two Gaussian functions is, however, enough to generate such patterns, and the reason why the nested patterns emerges is clear from the FT of the kernel shape. Therefore, if it is possible to translate the property of a given molecular network into a kernel shape, the behaviours of different models can be addressed in a unified method.

According to the simulation results from the KT model (Figs. 4–6), the conditions of stable pattern formation are quite simple: the integrated value of the 2D kernel is near zero, and the FT of the kernel has upward peaks. Concerning to the variety of the 2D pattern, Gierer and Meinhardt suggested that the saturation of activator synthesis is the key to change the spots to stripe and network (Meinhardt, 1982). However, this suggestion was not tested with rigorous mathematical analysis. With the KT model, the type of 2D pattern generated (spots,

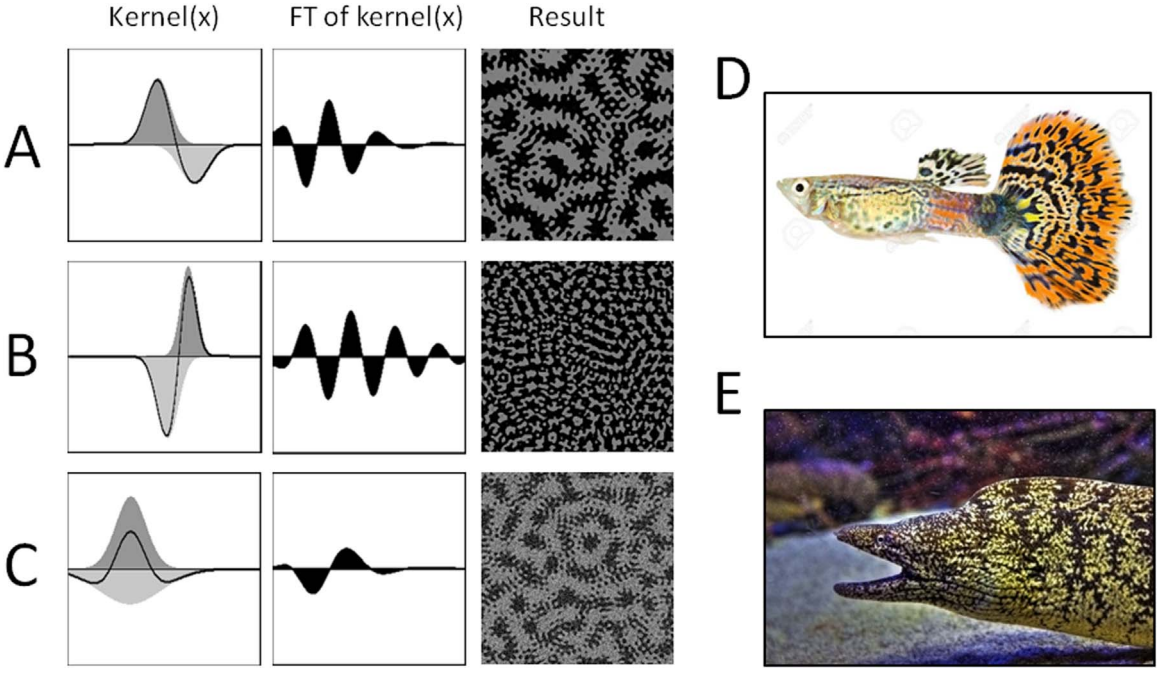

Fig. 7. Nested patterns generated by the KT model and examples of nested patterns in the skin of fish. A, B and C: Three different types of the kernels and the resulting patterns. D: An artificial line of guppy. E: Japanese common eel. See Parameter Settings for details. Random pattern is used as the initial condition.

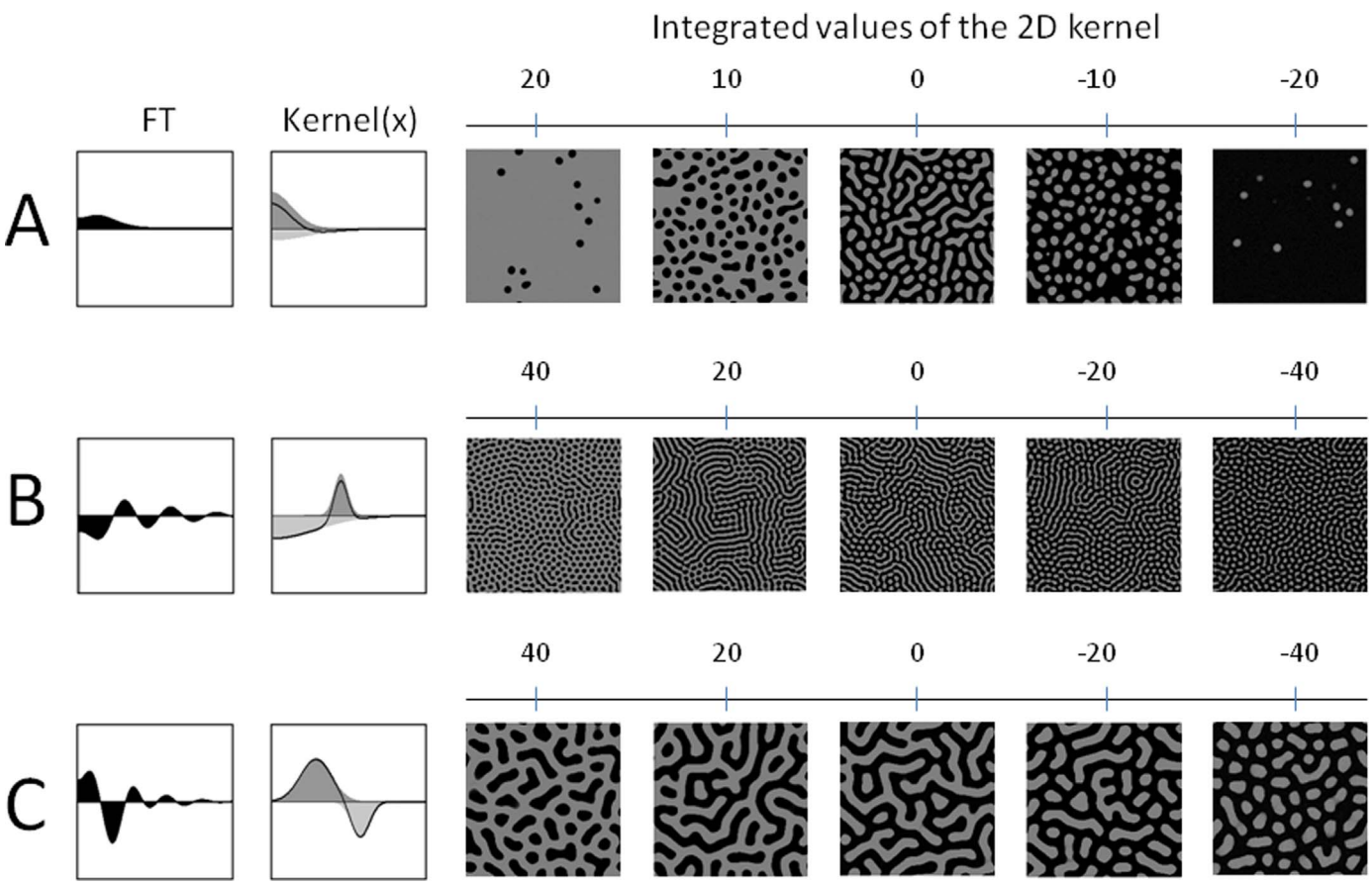

Fig. 8. Relationship between the integrated values of the 2D kernel (noted above each pattern) and the generated pattern. Five resulting 2D patterns calculated with the integrated values (upper) are shown for the kernel A, B and C. With this small difference of the integrated values of 2D kernel, the graph of FT and Kernel (x) looks almost identical. FT: Fourier Transform of the kernel shapes. For the Gaussian parameters of each kernel, see the list of parameter settings.

stripes, or networks) depends almost entirely on the integrated value of the 2D kernel. Although more mathematically strict verification should be performed in future studies, these simple conditions would be useful to understand the principle of pattern formation in real systems.

5. Conclusion

The properties of the KT model described above can complement the weaknesses identified in the pre-existing mechanistic models for autonomous pattern formation. I hope that the kernel-based method presented here will contribute to the progression of our understanding of biological pattern formation.

Competing interest

I have no competing interest.

Funding

This study was supported by JST, CREST, Grant number 12101628 and MEXT, Grant-in-Aid for Scientific Research, Grant number 15H05864.

Simulation program and the parameter sets used in the study

The simulation program was coded with Processing2.0 (Massachusetts Institute of Technology).

The compiled program will be distributed from the journal HP and the institute HP of Kondo.

The kernel function was defined as follows, where x is the distance between the cells:

Kernel[*x*]=ActivatorKernel[*x*]+InhibitorKernel[*x*]
ActivatorKernel[*x*]=ampA/sqrt(2*PI)*exp(-(sq((*x*-distA)/widthA)/2))
InhibitorKernel[*x*]=ampI/sqrt(2*PI)*exp(-(sq((*x*-distI)/widthI)/2))

The six parameters (ampA, ampI, widthA, widthI, dispA, and dispI) that determine the shape of the kernel are changed by the control sliders. The FT of the kernel, 3D kernel shape, and integrated value of the 2D kernel are automatically calculated when the parameter values are changed.

Pushing the “start-calculation” and “stop-calculation” buttons starts and stops the calculation, respectively. The “random-pattern” button gives a random value (0–1) to each cell. The “clear-the-field” button gives a value of 0 to each cell. Clicking the mouse on the calculation field gives a value of 0.5 to the cell at the position of the cursor.

Parameter settings.

	ampA	ampI	widthA	widthI	distA	distI	2D integrated
Fig. 4C left	20.267	−2.133	1.817	5.835	0	0	−14.119
Fig. 4C centre	21.971	−2.133	1.817	5.835	0	0	−0.017
Fig. 4C	250.67	−2.133	1.817	5.835	0	0	25.604

right							
Fig. 5 upper	22.4	−8	2.748	1.278	0	6.7	−0.398
Fig. 5 lower	−22.4	8	2.748	1.278	0	67	−0.398
Fig. 6A	15.275	−11.733	1.082	0.886	4.4	7	−0.318
Fig. 6B	12.656	−18.133	1.082	0.886	6.8	5.799	−0.413
Fig. 7A	17.192	−13.333	1.18	1.18	8.3	10.7	0.2
Fig. 7B	21.085	−19.733	0.739	0.935	10.3	8.7	−0.158
Fig. 7C	16.869	−5.867	1.229	3.872	5.9	6.1	24.6
Fig. 8A 20	14.287	−3.733	2.601	4.855	0	0	21.642
Fig. 8A 10	13.61	−3.733	2.601	4.855	0	0	10.246
Fig. 8A 0	13	−3.733	2.601	4.855	0	0	−0.11
Fig. 8A −10	12.413	−3.733	2.601	4.855	0	0	−10.59
Fig. 8A −20	11.827	−3.733	2.601	4.855	0	0	−20.001
Fig. 8B 40	13.652	−7.466	0.886	5.835	8.9	0	39.96
Fig. 8B 20	13.251	−7.466	0.886	5.835	8.9	0	20.076
Fig. 8B 0	12.844	−7.466	0.886	5.835	8.9	0	−0.072
Fig. 8B −20	12.443	−7.466	0.886	5.835	8.9	0	−19.956
Fig. 8B −40	12.038	−7.466	0.886	5.835	8.9	0	−39.97
Fig. 8C 40	14.182	−11.733	2.013	1.18	5.78	11.5	40.18
Fig. 8C 20	13.908	−11.733	2.013	1.18	5.78	11.5	20.032
Fig. 8C 0	13.634	−11.733	2.013	1.18	5.78	11.5	−0.022
Fig. 8C −20	13.356	−11.733	2.013	1.18	5.78	11.5	−20.468
Fig. 8C −40	13.089	−11.733	2.013	1.18	5.78	11.5	−40.034

Acknowledgement

I thank professors Takeshi Miura, Yoshihiro Tanaka and Ei Shin-ichiro for critical discussions and suggestions.

References

Belintsev, B.N., Beloussov, L.V., Zaraisky, A.G., 1987. Model of pattern formation in epithelial morphogenesis. J. Theor. Biol. 129, 369-94.

Blanchedeau, P., Boissonade, J., De Kepper, P., 2000. Theoretical and experimental studies of spatial bistability in the chlorine-dioxide-iodide reaction. Physica D 147, 17.

Budrene, E.O., Berg, H.C., 1995. Dynamics of formation of symmetrical patterns by chemotactic bacteria. Nature 376, 49–53. http://dx.doi.org/10.1038/376049a0.

De Joussineau, C., Soule, J., Martin, M., Anguille, C., Montcourrier, P., Alexandre, D., 2003. Delta-promoted filopodia mediate long-range lateral inhibition in Drosophila. Nature 426, 555–559. http://dx.doi.org/10.1038/nature02157.

Economou, A.D., Green, J.B., 2014. Modelling from the experimental developmental biologists viewpoint. Semin Cell Dev. Biol. 35, 58–65. http://dx.doi.org/10.1016/j.semcdb.2014.07.006.

Gierer, A., Meinhardt, H., 1972. A theory of biological pattern formation. Kybernetik 12, 30–39.

Green, J.B., Sharpe, J., 2015. Positional information and reaction-diffusion: two big ideas in developmental biology combine. Development 142, 1203–1211. http://dx.doi.org/10.1242/dev.114991.

Hamada, H., 2012. In search of Turing in vivo: understanding Nodal and Lefty behavior. Dev. Cell 22, 911–912. http://dx.doi.org/10.1016/j.devcel.2012.05.003.

Hamada, H., Watanabe, M., Lau, H.E., Nishida, T., Hasegawa, T., Parichy, D.M., Kondo, S., 2014. Involvement of Delta/Notch signaling in zebrafish adult pigment stripe patterning. Development 141, 318–324. http://dx.doi.org/10.1242/dev.099804.

Inaba, M., Yamanaka, H., Kondo, S., 2012. Pigment pattern formation by contact-dependent depolarization. Science 335, 677. http://dx.doi.org/10.1126/science.1212821.

Kondo, S., Asa, R., 1995. A reaction-diffusion wave on the skin of the marine angelfish Pomacanthus. Nature 376, 765–768.

Kondo, S., Miura, T., 2010. Reaction-diffusion model as a framework for understanding biological pattern formation. Science 329, 1616–1620. http://dx.doi.org/10.1126/science.1179047.

Liu, R.T., Liaw, S.S., Maini, P.K., 2006. Two-stage Turing model for generating pigment patterns on the leopard and the jaguar. Phys. Rev. E Stat. Nonlin Soft Matter Phys. 74, 011914. http://dx.doi.org/10.1103/PhysRevE.74.011914.

Maini, P., 2004. The impat of Turing's work on pattern formation in biology. Math. Today 40, 2.

Maini, P.K., Baker, R.E., Chuong, C.M., 2006. Developmental biology. The Turing model comes of molecular age. Science 314, 1397–1398. http://dx.doi.org/10.1126/science.1136396.

Marcon, L., Diego, X., Sharpe, J., Muller, P., 2016. High-throughput mathematical analysis identifies Turing networks for patterning with equally diffusing signals. Elife 5. http://dx.doi.org/10.7554/eLife.14022.

Meinhardt, H., 1982. Models of Biological Pattern Formation. Academic Press, London.

Meinhardt, H., 1995. Dynamics of stripe formation 376, 2.

Meinhardt, H., 2009. The Algorithmic Beauty of Sea Shells. Springer-Verlag, Berlin, Heidelberg.

Miura, T., 2007. Modulation of activator diffusion by extracellular matrix in Turing system. RIMS Kyokaku Bessatsu B3, 12.

Muller, P., Rogers, K.W., Jordan, B.M., Lee, J.S., Robson, D., Ramanathan, S., Schier, A.F., 2012. Differential diffusivity of Nodal and Lefty underlies a reaction-diffusion patterning system. Science 336, 721–724. http://dx.doi.org/10.1126/science.1221920.

Murray, J., 2001. Matheatical Biology. Springer, USA.

Nakamasu, A., Takahashi, G., Kanbe, A., Kondo, S., 2009. Interactions between zebrafish pigment cells responsible for the generation of Turing patterns. Proc. Natl. Acad. Sci. USA 106, 8429–8434. http://dx.doi.org/10.1073/pnas.0808622106.

Oster, G.F., 1988. Lateral inhibition models of developmental processes. Math. Biosci. 90, 256–286. http://dx.doi.org/10.1016/0025-5564(88)90070-3.

Ouyang, Q., Swinney, H., 1991. Transition from a uniform state to hexagonal and striped Turing patterns. Nature 352, 3.

Sagar, Prols, F., Wiegreffe, C., Scaal, M., 2015. Communication between distant epithelial cells by filopodia-like protrusions during embryonic development. Development 142, 665–671. http://dx.doi.org/10.1242/dev.115964.

Sheth, R., Marcon, L., Bastida, M.F., Junco, M., Quintana, L., Dahn, R., Kmita, M., Sharpe, J., Ros, M.A., 2012. Hox genes regulate digit patterning by controlling the wavelength of a Turing-type mechanism. Science 338, 1476–1480. http://dx.doi.org/10.1126/science.1226804.

Swindale, N.V., 1980. A model for the formation of ocular dominance stripes. Proc. R. Soc. Lond. B Biol. Sci. 208, 243–264.

Turing, A., 1952. The chemical basis of morphogenesis. Philos. Trans. R. Soc. Lond. Ser. B 237, 36.

Vasilopoulos, G., Painter, K.J., 2016. Pattern formation in discrete cell tissues under long range filopodia-based direct cell to cell contact. Math. Biosci. 273, 1–15. http://dx.doi.org/10.1016/j.mbs.2015.12.008.

Wearing, H.J., Owen, M.R., Sherratt, J.A., 2000. Mathematical modelling of juxtacrine patterning. Bull. Math. Biol. 62, 293–320. http://dx.doi.org/10.1006/bulm.1999.0152.

Yamaguchi, M., Yoshimoto, E., Kondo, S., 2007. Pattern regulation in the stripe of zebrafish suggests an underlying dynamic and autonomous mechanism. Proc. Natl. Acad. Sci. USA 104, 4790–4793. http://dx.doi.org/10.1073/pnas.0607790104.

Yamanaka, H., Kondo, S., 2014. In vitro analysis suggests that difference in cell movement during direct interaction can generate various pigment patterns in vivo. Proc. Natl. Acad. Sci. USA 111, 1867–1872. http://dx.doi.org/10.1073/pnas.1315416111.